

Three-dimensional numerical investigation of electron transport with rotating spoke in a cylindrical anode layer Hall plasma accelerator

D. L. Tang,^{1,a)} S. F. Geng,¹ X. M. Qiu,¹ and Paul K. Chu²

¹Southwestern Institute of Physics, Chengdu 610041, China

²Department of Physics and Materials Science, City University of Hong Kong, Tat Chee Avenue, Kowloon, Hong Kong

(Received 24 May 2012; accepted 13 July 2012; published online 30 July 2012)

The effects of increased magnetic field and pressure on electron transport with a rotating spoke in a cylindrical anode layer Hall plasma accelerator are investigated by three-dimensional particle-in-cell numerical simulation. The azimuthal rotation of electron transport with the spoke has a frequency of 12.5 MHz. It propagates in the direction of the $E \times B$ drift at a speed of $\sim 1.0 \times 10^6$ m/s (about 37% of the $E \times B$ drift speed). Local charge separation occurs because the azimuthal local electron density concentration is accompanied by an almost uniform azimuthal ion distribution. The non-axisymmetrical electron density concentration and axisymmetrical ion distribution introduce two azimuthal electric fields with opposite directions in the plasma discharge region. The axial electron shear flow is excited under the additional $E_\theta \times B$ field. The anomalous electron transport with the rotating spoke may be attributed to the axial electron shear flow induced by the two azimuthal electric fields with opposite directions as a result of the azimuthal local electron density concentration. © 2012 American Institute of Physics. [<http://dx.doi.org/10.1063/1.4740066>]

I. INTRODUCTION

The plasma discharge in $E \times B$ fields has many applications, such as magnetically confined fusion, Penning discharge ion source, magnetron sputtering, and Hall plasma accelerator. The electron transport characteristics in plasma discharge in the presence of $E \times B$ fields are very important to the plasma efficiency and fluctuation especially in a Hall plasma accelerator. Although there have been many studies on Hall plasma accelerators, several physical phenomena such as the electron transport mechanism are still not fully understood. In particular, the level of electron transport across the $E \times B$ fields cannot be explained by the classical collision mechanism. Some anomalous electron transport mechanisms such as Bohm diffusion,¹ near wall conductivity,² rotating spoke,³ and interaction of electrons with azimuthal wave of electric field⁴ were investigated in annular and cylindrical Hall plasma accelerator. The rotating spoke, which is an important fluctuation phenomenon in $E \times B$ fields, was found in the Hall plasma accelerator in 1966.⁵ The light emission characteristics in the $E \times B$ plasma discharge were also observed in other Hall plasma accelerators^{6,7} as well as magnetron sputtering devices.^{8,9}

An electrostatic Langmuir probe is often used to measure the plasma potential and density in the study of anomalous electron diffusion. Although an electrostatic probe perturbs the plasma, the Langmuir probe is still used because of a lack of alternative measurement methods. At the same time, numerical simulation is commonly employed to describe plasma discharge characteristics. Recently, much effort has been made to model the plasma behavior in Hall plasma accelerators by, for example, the fluid model,^{10–12}

PIC (particle-in-cell) model,¹³ and hybrid-PIC model.¹⁴ The near field plume was described by a two-dimensional (2D) hybrid-PIC model,¹⁵ and the interactions between the plasma and wall were simulated by Sommier *et al.* also based on a 2D hybrid-PIC model.¹⁶ The sheath formation and expansion were investigated using a 2D hydrodynamic approach by Keidar *et al.*¹⁷ and the high-frequency electron drift instability by Ducrocq *et al.* using PIC simulation as well.¹⁸ However, in the two-dimensional model, the azimuthal dynamics is not considered and the electron transport characteristics along the $E \times B$ direction cannot be included. In our previous work, we applied three-dimensional PIC with Monte Carlo collisions (MCCs) to simulate the discharge characteristics of the cylindrical anode layer Hall plasma accelerator to account for the $E \times B$ drift. The simulation results revealed a threshold voltage corresponding to the maximum ionization cross section which was the same as that determined experimentally.¹⁹ The electron and ion distributions were uniform along the azimuthal $E \times B$ direction and no density concentration and plasma fluctuations were observed. In order to further understand the electron transport characteristics in the presence of different $E \times B$ fields, we extend the electric and magnetic field values and gas pressure in this study and electron transport with rotating spoke is observed.

II. NUMERICAL SIMULATION

The simulation is performed by the 3D PIC method using the software VORPAL by Tech-X Corporation. The anode layer Hall plasma accelerator used in our experiments and simulation is schematically illustrated in Fig. 1.

The model is based on the 3D Cartesian coordinates and the modeled volume is 50 mm \times 50 mm \times 50 mm. In the simulation, the argon pressure is increased to 4×10^{-2} Pa based on previous experimental data and the magnetic field strength

^{a)}Electronic mail: tangdeli@263.net.

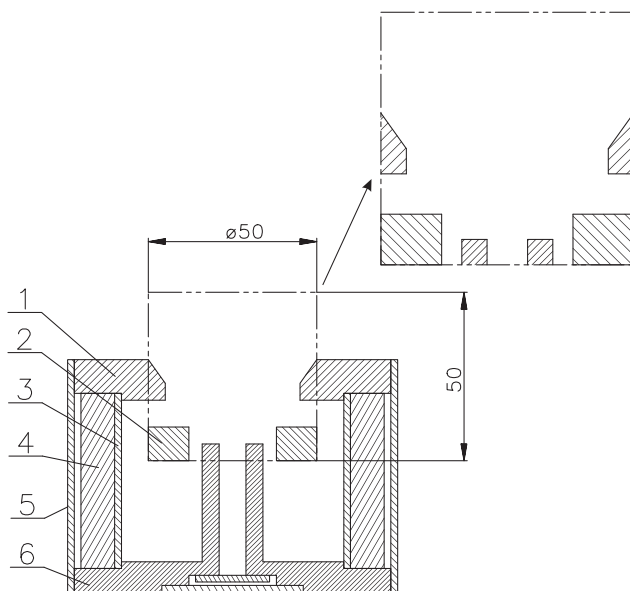


FIG. 1. Schematic cross-sectional diagram of the cylindrical anode layer Hall plasma accelerator and simulated parts: (1) cathode/outer magnetic pole, (2) anode, (3) inner shield, (4) permanent magnet, (5) outer shield, and (6) cathode/inner magnetic pole. Reprinted with permission from Phys. Plasmas **19**, 043507 (2012). Copyright 2012 American Institute of Physics.

is enlarged by 1.67. Here, the pressure 4×10^{-2} Pa means a mass flow of 16 SCCM under the condition of vacuum vessel and pumps described in Ref. 19. The discharge voltage applied to the model is 600 V and particle collision is handled by MCC. The type of collisions includes electron-neutral collisions (ionization, excitation, and elastic scattering) as well as ion-neutral collisions (charge exchange and elastic scattering). All the collisional cross section data are the VORPAL built-in data which are based on a parameterized fit from Martin Reiser, Theory and Design of Charged Particle Beams (Wiley, New York, 1994).

The other details are as follows: The size of each cell is $1 \text{ mm} \times 1 \text{ mm} \times 1 \text{ mm}$ indicating that there are 125 000 cells in the mesh. A total of 27 000 macroparticles for electrons and 27 000 ones for ions are put into the center of the model. In the simulation, some of them will be lost because of collisions between particles and the wall or because they escape from the simulated region. Some new ones are added to the model because of ionization. The simulation is conducted in a single thread (serial mode) with time step 1×10^{-10} s and the CPU time taken is 10 199 s.

III. RESULTS AND DISCUSSION

The front view of the electron distributions at different time is illustrated in Fig. 2. The non-axisymmetrical electron distribution is clearly shown in Fig. 2 and the electron concentration position is also changed at different time. The outline of the electron transport with the rotating spoke is revealed, and it is similar to the images captured by a high-speed camera.^{3,20} Fig. 2 shows the half cycle of electron transport with the spoke (from (a) to (f)) at about 4×10^{-8} s, indicating that the frequency of the rotating spoke is about 12.5 MHz. The speed of the rotating spoke is

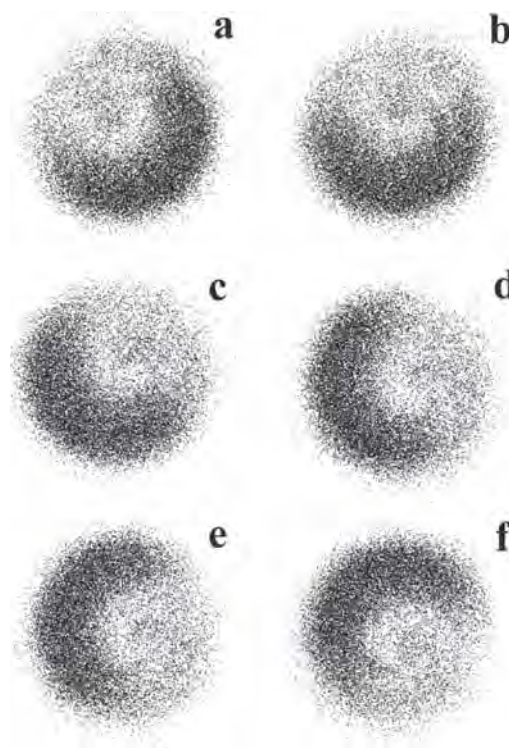


FIG. 2. Front view of the electron distributions with different times. These six images (a–f) show half a cycle of electron condensation rotation.

$\sim 1.0 \times 10^6$ m/s, which is about 37% of the Hall drift speed obtained by E/B .

The electron distributions in space at different magnetic field and gas pressure values are shown in Figs. 3(a) and 3(b). Here, the accelerator model is clipped along the center line to reveal the 3D electron distributions. A visible azimuthal electron concentration is observed from Fig. 3(a) and the electron distribution is azimuthally uniform in Fig. 3(b). No obvious azimuthal electron concentration is found from the simulation results based on our experimental data at 105 G on the anode surface and gas pressure of 2×10^{-2} Pa. When we change the magnetic field to 175 G and gas pressure to 4×10^{-2} Pa, a significant electron concentration is found along the azimuthal direction. On the other hand, the ion distributions are almost uniform along the azimuthal direction at different magnetic field and gas pressure and there is no azimuthal ion concentration. It is thus concluded that local charge separation occurs because of the azimuthal electron density concentration accompanied by almost uniform azimuthal ion distribution. Therefore, the azimuthal electric field E_θ exists in the anode layer Hall plasma accelerator. It means that the electron transport with the rotating spoke introduces an azimuthal electric field E_θ . The azimuthal electric field E_θ has also been observed from other Hall thrusters.^{5,20}

The rotating spoke is a collective effect of azimuthal electron transport, which is consistent with light emissions images acquired on a high speed camera. The electron transport with the rotating spoke exists not only near the anode but also throughout the entire main discharge channel. The equipotential contours of the different axial positions for

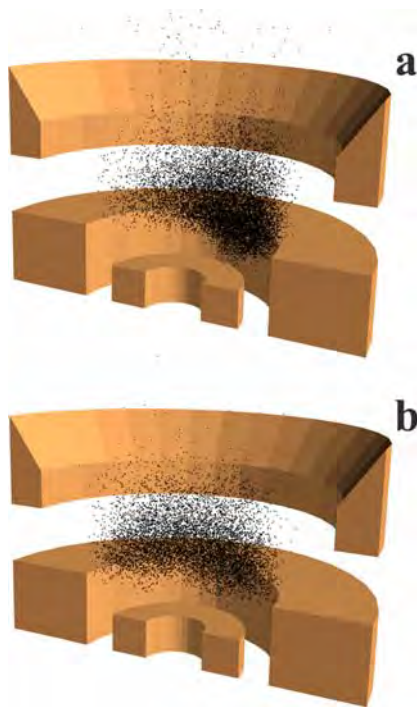


FIG. 3. Electron distribution in the cylindrical anode layer Hall plasma accelerator. (a) Electron distribution with 175 G and 4×10^{-2} Pa; (b) electron distribution with 105 G and 2×10^{-2} Pa.

Fig. 2(d) are shown in Fig. 4. The distances to the anode surface are 1 mm, 2 mm, 3 mm, and 4 mm. The potential maps show the existence of the azimuthal electric field in different axial planes. It demonstrates the spoke feature and also rotates along the azimuthal direction at the same speed as the spoke transport. In our simulation, the azimuthal electric field E_θ is about 10–20 V/mm.

The azimuthal electric field E_θ can cause an axial drift of the electrons because of the magnetic field in the additional $E_\theta \times B$ field. It increases the electron mobility in the axial direction. In our simulation, electrons occupy the larger axial region when the spoke takes place and it can be easily observed from Fig. 3(a).

Considering the azimuthal integral for E_θ along an electron closed drift path with radius r , the integral is zero due to the closed path:

$$\oint E_\theta \cdot dl = \int_0^{2\pi} E_\theta \cdot r \cdot d\theta = 0. \quad (1)$$

Equation (1) shows that E_θ has both positive and negative values along the closed drift path or E_θ has two opposite directions. Fig. 4 also shows that E_θ has two opposite directions along the azimuthal direction due to the azimuthal local electron density concentration, which introduces the electron axial drift along opposite directions upstream and

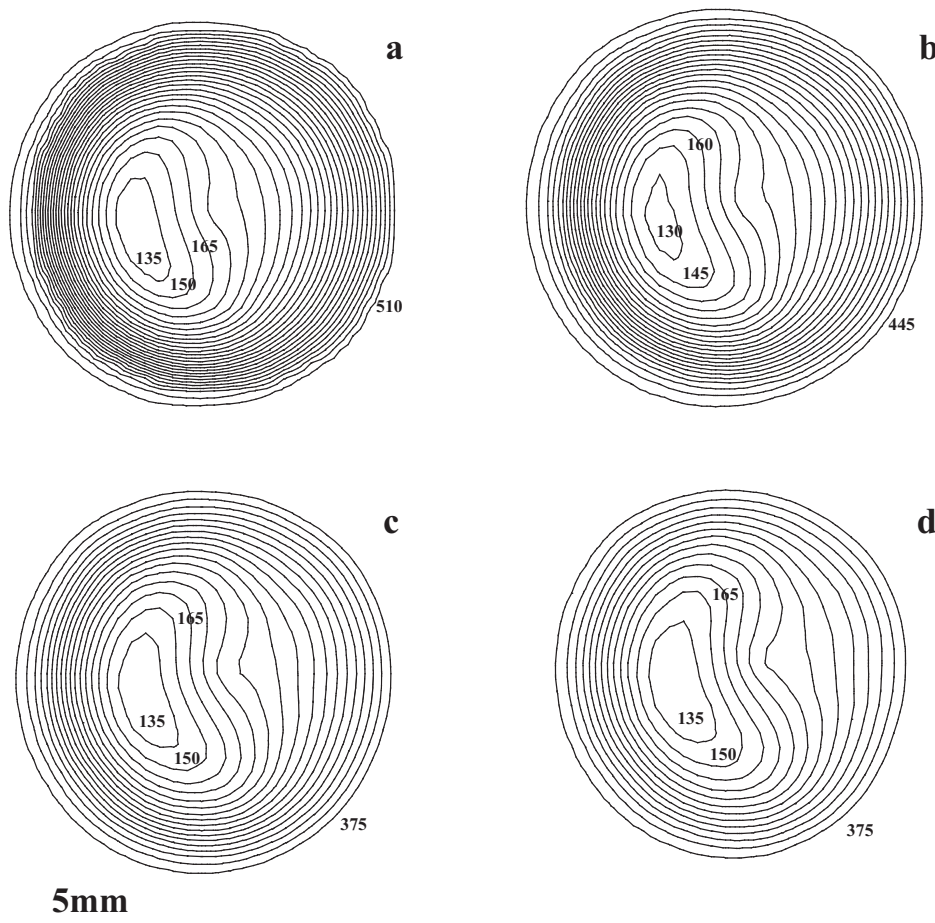


FIG. 4. Equipotential contours in different plane of the spoke (the unit of the labels is volt). (a) 1 mm, (b) 2 mm, (c) 3 mm, and (d) 4 mm from the anode surface.

downstream. Therefore, the axial electron shear flow is excited. The electron drift upstream contributes to the anode current and it is consistent with the spoke current experimentally measured by the segment anode.²⁰ The electron drift downstream escapes from the discharge region and acts as the electron background for ion extraction. The axial local charge separation induced by the axial shear electron flow may be compensated by the azimuthal electron transport, finally resulting in the azimuthal electric field rotation and electron transport with the rotating spoke. It means that the anomalous electron transport with the rotating spoke may be attributed to the axial electron shear flow induced by two azimuthal electric fields with opposite directions existing due to the azimuthal local electron density concentration.

In the present simulation, the pressure and magnetic field are both increased, but the critical parameter is the magnetic field for the rotating spoke. In another simulation, it is proven that the rotating spoke exists all the same at low pressure, if the high magnetic field is kept. The rotating spoke in the high magnetic field looks obvious and clear. Under a small magnetic field, the rotating spoke does not disappear, but rather it becomes not apparent and light. We do not find a magnetic field threshold for the appearance of the rotating spoke.

The non-neutral property of the plasmas in the Hall plasma accelerator must be considered due to the large mean free path, strongly magnetized electrons, and non-magnetized ions. We consider that the rotating spoke is induced by the diocotron instability, since the diocotron instability is one of the most ubiquitous instabilities in non-neutral plasmas.²¹ However, the rotating spoke is more complex than the ordinary two-dimensional diocotron instability because the velocity shear of the electron stream exists in both the radial and the axial directions.

IV. CONCLUSION

Electron transport with a rotating spoke is observed from three-dimensional particle-in-cell simulation of a cylindrical anode layer Hall plasma accelerator and the phenomenon is investigated under increasing magnetic field and pressure. The azimuthal rotation of the electron transport with the spoke has a frequency of 12.5 MHz. It propagates in the direction of the $E \times B$ drift at a speed of $\sim 1.0 \times 10^6$ m/s

(about 37% of the $E \times B$ drift speed). Local charge separation occurs because of the azimuthal electron density concentration accompanied by an almost uniform azimuthal ion distribution. The non-axisymmetrical electron concentration and axisymmetrical ion distribution introduce two azimuthal electric fields with opposite directions in the plasma discharge region. The axial electron shear flow is excited under the additional $E_\theta \times B$ field. The anomalous electron transport with the rotating spoke may be attributed to the axial electron shear flow induced by two azimuthal electric fields with opposite directions.

ACKNOWLEDGMENTS

This work was supported by the National Natural Science Foundation of China under Grant No. 10975050 and Hong Kong Research Grants Council (RGC) Special Equipment Grant (SEG) No. CityU SEG_CityU05.

- ¹N. B. Meezan, W. A. Hargus, and M. A. Cappelli, *Phys. Rev. E* **63**, 026410 (2001).
- ²A. I. Morozov and V. V. Savel'ev, *Plasma Phys. Rep.* **27**, 570 (2001).
- ³J. B. Parker, Y. Raitses, and N. J. Fisch, *Appl. Phys. Lett.* **97**, 091501 (2010).
- ⁴A. N. Vesselovzorov, E. D. Dlougach, A. A. Pogorelov, E. B. Svirskiy, and V. A. Smirnov, in Proceedings of the IEPC-2011-060, 2011.
- ⁵G. S. Janes, *Phys. Fluids* **9**, 1115 (1966).
- ⁶P. J. Lomas and J. D. Kilkenny, *Plasma Phys.* **19**, 329 (1977).
- ⁷E. Chesta, C. M. Lam, N. B. Meezan, D. P. Schmidt, and M. A. Cappelli, *IEEE Trans. Plasma Sci.* **29**, 582 (2001).
- ⁸T. Ito and M. A. Cappelli, *IEEE Trans. Plasma Sci.* **36**, 1228 (2008).
- ⁹T. Ito and M. A. Cappelli, *Appl. Phys. Lett.* **94**, 211501 (2009).
- ¹⁰E. Y. Choueiri, *Phys. Plasmas* **8**, 5025 (2001).
- ¹¹M. Keidar, I. D. Boyd, and I. I. Beilis, *Phys. Plasmas* **8**, 5315 (2001).
- ¹²L. Dorf, V. Semenov, and Y. Raitses, *Appl. Phys. Lett.* **83**, 2551 (2003).
- ¹³F. Taccogna, S. Longo, M. Capitelli, and R. Schneider, *Contrib. Plasma Phys.* **47**, 635 (2007).
- ¹⁴K. Komurasaki and Y. Arakawa, *J. Propul. Power* **11**, 1317 (1995).
- ¹⁵I. D. Boyd and J. T. Yim, *J. Appl. Phys.* **95**, 4575 (2004).
- ¹⁶E. Sommier, M. K. Scharfe, N. Gascon, M. A. Cappelli, and E. Fernandez, *IEEE Trans. Plasma Sci.* **35**, 1379 (2007).
- ¹⁷M. Keidar, I. D. Boyd, and I. I. Beilis, *Phys. Plasmas* **11**, 1715 (2004).
- ¹⁸A. Ducrocq, J. C. Adam, A. Héron, and G. Laval, *Phys. Plasmas* **13**, 102111 (2006).
- ¹⁹S. F. Geng, X. M. Qiu, C. M. Cheng, P. K. Chu, and D. L. Tang, *Phys. Plasmas* **19**, 043507 (2012).
- ²⁰C. L. Ellison, Y. Raitses, and N. J. Fisch, *Phys. Plasmas* **19**, 013503 (2012).
- ²¹R. C. Davison, *Physics of Nonneutral Plasmas*, 2nd ed. (Imperial College Press/World Scientific, London, UK, 2001), p. 289.